Scientific report - 2015 - project IDEI-0153: "ADVANCED STUDIES ON STRUCTURE AND DYNAMICS OF EXOTIC NUCLEI"
I. Stellar weak interaction rates and shape coexistence for ^{68}Se and ^{72}Kr waiting points

Self-consistent microscopic approaches capable of describing the experimentally accessible properties of nuclei are needed to predict nuclear characteristics beyond the experimental reach required by nuclear astrophysics as well as other nuclear applications. In particular, properties of exotic nuclei difficult to explore experimentally are relevant for astrophysical scenarios of explosive phenomena like X-ray bursts [1, 2]. This is the case of nuclei in the A$\sim$70 mass region involved in the nucleosynthesis rapid proton-capture (rp) process.

The description of the Gamow-Teller (GT) strength distributions for the beta decay of nuclei close to the proton-drip line in this mass region meets the difficulty of treating self-consistently the shape coexistence and mixing, which dominate the structure of both even-even parent and odd-odd daughter nucleus, varying strongly with particle number, angular momentum and excitation energy. For nuclei close to the N=Z line the problem is even more complicated by the competition between the neutron-proton and like-nucleon pairing correlations expected to influence the behaviour of these nuclei significantly. Previous theoretical investigations [3, 4] suggested that in this mass region the β-decay strength distributions depend sensitively on the nuclear shape. Stellar weak interaction rates have been evaluated for waiting point nuclei along the rp-process path in A$\sim$70 region based on QRPA approach using different nucleon-nucleon interactions [5]. An essential issue at the temperatures (1 - 3 GK) and densities ($10^6 - 10^7 g/cm^3$) characteristic for the rp process is the contribution of the thermally populated low-lying 0^+ and 2^+ states. The realistic description of the structure of these states in parent nuclei as well as the states in daughter nuclei dominated by shape mixing requires beyond-mean-field methods.

The coexistence phenomena dominating the structure and dynamics of medium mass proton-rich and neutron-rich nuclei have been intensively investigated within the *complex* Excited Vampir approach and many predictions that emerged have been experimentally confirmed. The present study is the first atempt at a completely self-consistent calculation of the stellar weak interaction rates for ^{68}Se and ^{72}Kr waiting-point nuclei at densities $\rho = 10^4 - 10^7 g/cm^3$ and temperatures $T = 10^8 - 10^{10} K$ using the *complex* Excited Vampir approach. The influence of the shape mixing is investigated using different effective interactions and rather large model spaces.

The *complex* Excited Vampir model uses Hartree-Fock-Bogoliubov (HFB) vacua as basic building blocks. The underlying HFB transformations are essentially *complex* and do mix proton- with neutron-states as well as states of different parity and angular momentum beeing restricted by time-reversal and axial symmetry. The broken symmetries of these vacua (nucleon numbers, parity, total angular momentum) are restored by projection techniques and the resulting symmetry-projected configurations are used as test wave functions in chains of successive variational calculations to determine the underlying HFB transformations as well as the configuration mixing ([3] and references therein). The HFB vacua of the above type account for arbitrary two-nucleon correlations and thus simultaneously describe like-nucleon as well as isovector and isoscalar proton-neutron pairing including natural- (e.g., with $I^\pi = 0^+$) and unnatural-parity (e.g., with $I^\pi = 1^+$) two-body correlations. Furthermore, the *complex* Excited Vampir model (EXVAM) allows the use of rather large model spaces and realistic effective interactions.

For nuclei in the $A \sim 70$ mass region we used a

^{40}Ca core and included the $1p_{1/2}$, $1p_{3/2}$, $0f_{5/2}$, $0f_{7/2}$, $1d_{5/2}$ and $0g_{9/2}$ oscillator orbits for both protons and neutrons in the valence space ('standard model space'). We start with an isospin symmetric basis and then introduce the Coulomb shifts for the proton single-particle levels resulting from the ^{40}Ca core by performing spherically symmetric Hartree-Fock calculations using the Gogny-interaction D1S in a 21 major-shell basis [3].

We present also results obtained using a much larger model space above the ^{40}Ca core built out of $1p_{1/2}$, $1p_{3/2}$, $0f_{5/2}$, $0f_{7/2}$, $2s_{1/2}$, $1d_{3/2}$, $1d_{5/2}$, $0g_{7/2}$, $0g_{9/2}$, and $0h_{11/2}$ oscillator orbits for both protons and neutrons in the valence space ('extended model space'). This large model space was succesfully used for the description of shape coexistence phenomena including Gamow-Teller beta decay for neutron-rich A$\sim$100 nuclei.

The effective two-body interaction is constructed from a nuclear matter G-matrix based on the Bonn One-Boson-Exchange Potential (Bonn A/Bonn CD). This G-matrix was modified by adding short-range (0.707 fm) Gaussians in the T=1 and T=0 channels in order to enhance the pairing correlations. In addition the isoscalar interaction was modified by monopole shifts for the T=0 matrix elements of the form $\langle 0g_{9/2}0f; IT=0|\hat{G}|0g_{9/2}0f; IT=0\rangle$ involving protons and neutrons in the $0g_{9/2}$, $0f_{5/2}$, and $0f_{7/2}$ orbitals [3]. The Hamiltonian includes the two-body matrix elements of the Coulomb interaction between the valence protons. Replacing the Bonn A by the Bonn CD potential or extending the model space does not modify the characteristics of the Excited Vampir many-body configuration basis of each symmetry significantly, but the relative position of the projected differently deformed configurations in the intrinsic system is altered and, consequently, the shape mixing is changed for the states of the parent as well as of the independently calculated daughter nucleus.

We extended the previous studies on Gamow-Teller β decay of ^{68}Se [4] using the standard model space and the effective interactions obtained starting from Bonn A and Bonn CD potential. In the present work we calculated the lowest 2^+ state in ^{68}Se including in the Excited Vampir many-nucleon basis up to eight configurations. In ^{68}As we calculated the lowest 50 3^+ states and the lowest 21 2^+ states. The mixing of the differently deformed configurations in the intrinsic system in the structure of the yrast 2^+ state in ^{68}Se indicates 60% (41%) oblate content for Bonn A (Bonn CD) potential. Consequently, the spectroscopic quadrupole moment is changing from 3.5 efm^2 for Bonn A to -7.1 efm^2 for Bonn CD (effective extra charge of 0.3 e is used). A similar but not identical mixing has been found for the ground state of ^{68}Se where the amplitude of the oblate deformed configurations amounts to 62% (55%) for Bonn A (Bonn CD) potential [4]. Figure 1 illustrates the large variety of deformations displayed by the spectroscopic quadrupole moments of the lowest 30 3^+ states in ^{68}As and the change introduced replacing Bonn A by Bonn CD potential.

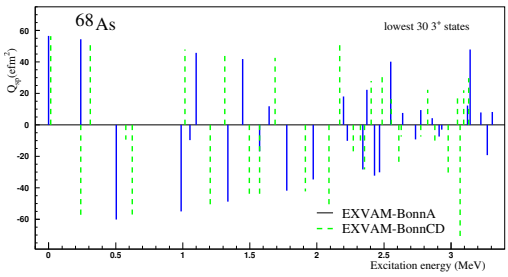

Figure 1: Spectroscopic quadrupole moments of the lowest 30 3^+ states in ^{68}As obtained within the *complex* Excited Vampir model using different effective interactions.

The characteristics of the projected Excited Vampir configurations are not significantly modified by replacing Bonn A with Bonn CD potential, but their mixing in the structure of the final wave functions is changed. Consequently, we can study the influence of the shape mixing on the Gamow-Teller strength distributions and finally on the stellar weak interaction rates. In Figure 2 are compared the accumulated Gamow-Teller strengths obtained using Bonn A and Bonn CD potential for the decay of the ground state and yrast 2^+ state in ^{68}Se to EXVAM 1^+, 2^+, and 3^+ states in ^{68}As. We calculated the half-life for the decay of the ground state of ^{68}Se by summing up the contributions up to 1^+ states in ^{68}As with excitation energies lying within the experimental beta window:

$$\frac{1}{T_{1/2}} = \frac{g_A^2}{D} \sum_i f(Z, E_i) |\left\langle 1_i^+ || \beta^+ || 0^+ \right\rangle|^2 \qquad (1)$$

where $f(Z, E_i)$ are the Fermi integrals. We use $D = 6146$ s and $g_A = 1.26$. The measured half-life

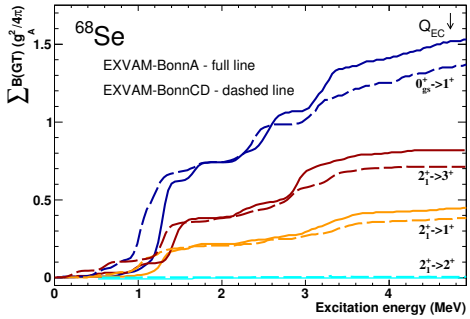

Figure 2: Gamow-Teller accumulated strengths for the decay of the ground state and yrast 2^+ state in ^{68}Se to the daughter states in ^{68}As obtained within *complex* Excited Vampir model using Bonn A and Bonn CD potential.

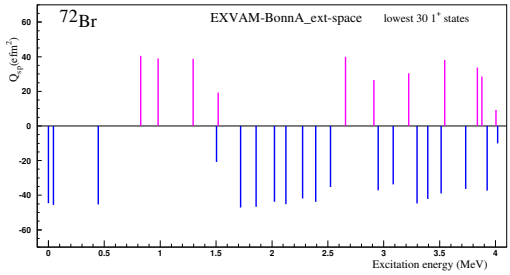

Figure 3: Spectroscopic quadrupole moments of the lowest 30 1^+ states in ^{72}Br obtained within the *complex* Excited Vampir model in the extended model space using Bonn A potential.

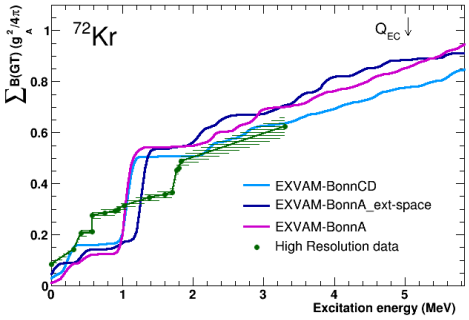

Figure 4: Gamow-Teller accumulated strengths for the decay of the ground state of ^{72}Kr obtained within *complex* Excited Vampir model in two different model spaces (see text) using Bonn A/Bonn CD potential are compared with high resolution results [6].

of ^{68}Se is 35.5(0.7) s, while the β-decay scheme is established up to 426 keV excitation energy from the whole beta window of Q_{EC} = 4730(310) keV. The EXVAM result for the terrestrial half-life is 48.8 (33.5) s using Bonn A (Bonn CD) potential [4].

For the ^{72}Kr waiting point nucleus we extended the previous investigations [3] calculating the Gamow-Teller distribution strengths for the decay of the ground state, the lowest excited 0^+ state and the yrast 2^+ state in the extended model space discussed above using the Bonn A potential. We calculated the lowest 0^+ and 2^+ states of the even-even ^{72}Kr parent nucleus and, independently, the 1^+, 2^+, and 3^+ states in the odd-odd ^{72}Br daughter nucleus. For the description of the 0^+ and 2^+ states of ^{72}Kr we included in the Excited Vampir many-nucleon basis eight EXVAM configurations, while for the description of the states in ^{72}Br we calculated the lowest 50 1^+ and 3^+ and the lowest 27 2^+ projected configurations. The results concerning the oblate-prolate mixing in the structure of the wave function for the ground state of ^{72}Kr indicate that 40% of the total amplitude is built out of oblate-deformed configurations (even if the lowest minimum is oblate-deformed in the intrinsic system), while the remaining 60% are made up by various prolate-deformed EXVAM configurations including almost spherical ones (3%). The first excited 0^+- and the yrast 2^+-state are dominated by oblate components (62% and 59%, respectively). The corresponding mixing in the standard model space indicates 66%, 37%, and 93% oblate content for the lowest two 0^+ states and the yrast 2^+ state, respectively.

In ^{72}Br the calculated 1^+, 2^+, and 3^+ states manifest variable, sometimes strong mixing of differently deformed oblate and prolate configurations in the intrinsic system as it has been found also in the standard model space [3]. To illustrate the large variety of deformations of the calculated states the spectroscopic quadrupole moments of the lowest 30 1^+ states are presented in Figure 3. As it was revealed by the structure of the states in ^{72}Kr the evolution of the mixing with increasing excitation energy for the daughter states in ^{72}Br is changing for the extended space with respect to that found in the standard space, too, while the characteristics of the EXVAM many-body configurations for each symmetry are not significantly changed.

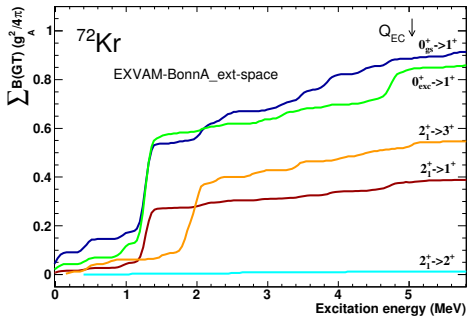

Figure 5: Gamow-Teller accumulated strengths for the decay of the ground state, first excited 0^+ state and yrast 2^+ state of ^{72}Kr to the daughter states in ^{72}Br obtained within *complex* Excited Vampir model using Bonn A potential in the extended model space.

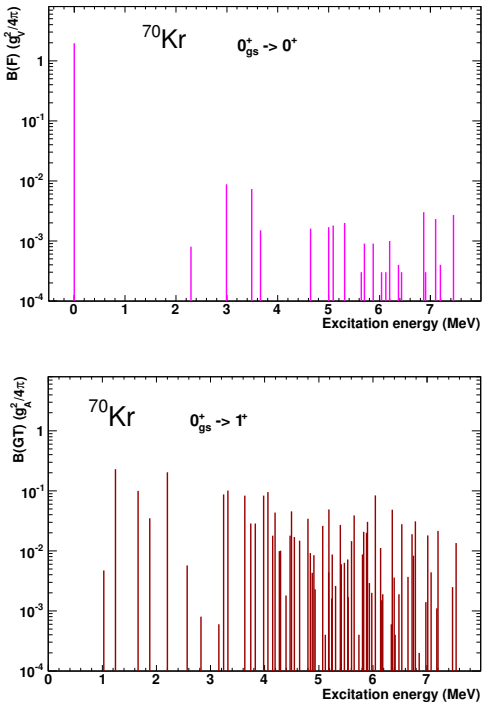

Figure 6: Fermi and Gamow-Teller strength distributions for the decay of the ground state in ^{70}Kr to daughter states in ^{70}Br obtained within the *complex* Excited Vampir model.

In Figure 4 we present the EXVAM Gamow-Teller accumulated strengths for the decay of the ground state of ^{72}Kr and compare with high resolution [6] results. In the same figure are presented the theoretical results obtained using an effective interaction based on Bonn A/Bonn CD potential in the standard model space [3] and the new results calculated in the extended model space using Bonn A potential. In Figure 5 are presented the Gamow-Teller accumulated strengths for the decay of the ground state, first excited 0^+ state and yrast 2^+ state of ^{72}Kr to the daughter 1^+, 2^+, and 3^+ states in ^{72}Br obtained within *complex* Excited Vampir model using the Bonn A potential in the extended model space. We calculated the half-life for the decay of the ground state of ^{72}Kr by summing up the contributions up to 1^+ states in ^{72}Br with excitation energies lying within the experimental Q_{EC}. The experimental value of the half-life for the decay of the ground state of ^{72}Kr is 17.1(2) s [6], whereas the Excited Vampir result is 20.8(20.7) s for the Bonn A potential in the standard (extended) model space and 18.9 s in the standard model space for the Bonn CD potential [3].

We also extend our study on the effect of shape mixing on the weak interaction rates for Z=N+2 ^{70}Kr and ^{74}Sr isotopes describing the low-lying 0^+ and 2^+ states in the parent nuclei and the corresponding daughter 0^+, 1^+, 2^+, and 3^+ states in ^{70}Br and ^{74}Rb, respectively, within the *complex* Excited Vampir model based on the effective interaction obtained from the charge-dependent Bonn CD potential and the adequate model space previously used to investigate the effect of the isospin mixing in the isovector triplets with A=70 and A=74. The Fermi and Gamow-Teller strength distribution for the decay of the ground state in ^{70}Kr to daughter states in ^{70}Br obtaind within the *complex* Excited Vampir model are prezented in Figure 6. The same as in Figure 6 but for ^{74}Sr is presented in Figure 7.

The general formalism to calculate weak interaction rates for a stellar environment has been introduced by Fuller et al. [1]. Since in the ranges of densities and temperatures relevant for the *rp* process the stellar beta decay and continuum electron capture are sensitive to the distribution of the Gamow-Teller strength a realistic treatment of the shape coexistence and mixing dominating the structure of the low-lying states of the waiting point nuclei and the corresponding daughter states is required. The

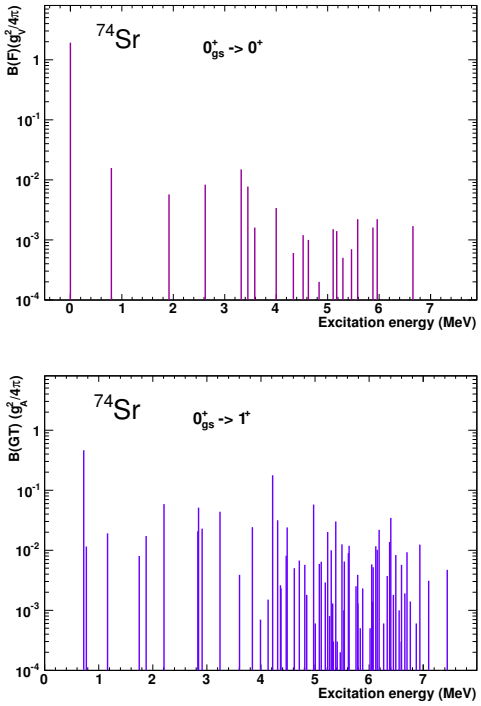

Figure 7: Fermi and Gamow-Teller strength distributions for the decay of the ground state in ^{74}Sr to daughter states in ^{74}Rb obtained within the *complex* Excited Vampir model.

rate for the weak processes is given by

$$\lambda^{\alpha} = \frac{ln2}{K} \sum_i \frac{(2J_i+1)e^{-E_i/(kT)}}{G(Z,A,T)} \sum_j B_{ij}\phi^{\alpha}_{ij}, \quad (2)$$

where α stays for the considered processes (β^+ decay and continuum electron capture), the constant K=6146 s, the sums in i and j run over the termally populated parent states i of spin J_i and excitation energy E_i and j daughter states, respectively. G is the partition function of the parent nucleus (Z,A) defined by $G(Z,A,T) = \sum_i (2J_i + 1)exp(-E_i/(kT))$. B_{ij} are the reduced matrix elements of the considered Gamow-Teller decay. The last factor ϕ^{α}_{ij} is the phase space integral for the two calculated processes, β^+ decay and continuum electron capture, given by

$$\begin{aligned}\phi^{\beta^+}_{ij} &= \int_1^{Q_{ij}} wp(Q_{ij}-w)^2 F(-Z+1,w) \\ &\times (1-S_p(w))(1-S_\nu(Q_{ij}-w))dw,\end{aligned} \quad (3)$$

$$\phi^{ec}_{ij} = \int_{w_l}^{\infty} wp(Q_{ij}+w)^2 F(Z,w) S_e(w)(1-S_\nu(Q_{ij}+w))dw, \quad (4)$$

where w is the total, rest mass and kinetic, energy of the electron or positron in units of $m_e c^2$, $p = \sqrt{w^2-1}$ is the momentum in units of $m_e c$, and Q_{ij} is the total energy available in β^+ decay in units of $m_e c^2$,

$$Q_{ij} = \frac{1}{m_e c^2}(M_p - M_d + E_i - E_j), \quad (5)$$

where M_p, M_d are the nuclear masses of the parent and daughter nucleus, respectively, whereas E_i, E_j are the excitation energies of the initial and final states. Depending on Q_{ij} the threshold is w_l=1 if $Q_{ij} > -1$, or $w_l = |Q_{ij}|$ if $Q_{ij} < -1$. The Fermi function, $F(Z,w)$, correcting the phase space integral for the Coulomb distortion of the electron or positron wave function near the nucleus is approximated by

$$F(Z,w) = 2(1+\gamma)(2pR)^{-2(1-\gamma)} \frac{|\Gamma(\gamma+iy)|^2}{|\Gamma(2\gamma+1)|^2} e^{\pi y} \quad (6)$$

where $\gamma = \sqrt{1-(\alpha Z)^2}$, $y = \alpha Z w/p$, α is the fine structure constant, and R is the nuclear radius. S_e, S_p and S_ν are the electron, positron, and neutrino distribution functions, respectively. In the

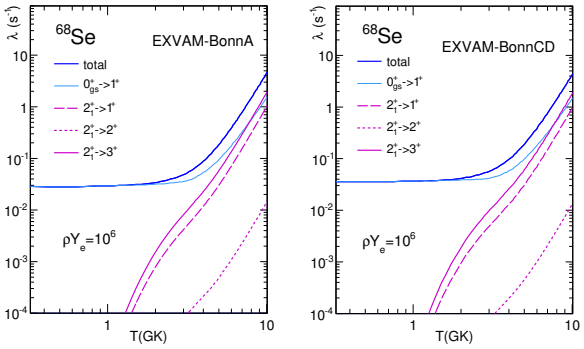

Figure 8: Decay rates (s^{-1}) of ^{68}Se as a function of temperature T (GK) for *rp*-process typical density ρY_e (mol/cm^3) obtained within *complex* Excited Vampir model using the Bonn A (left) and Bonn CD (right) potential. The total rate is decomposed into contributions from the decay of the ground state and yrast 2^+ state to the daughter states in ^{68}As.

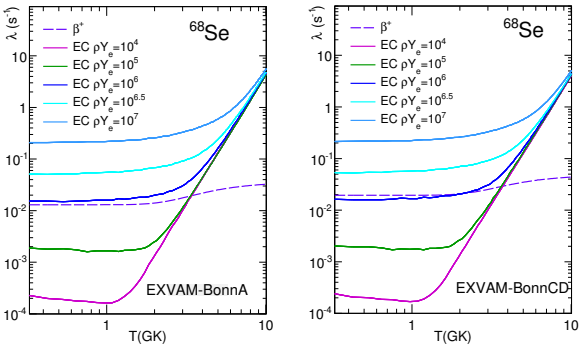

Figure 9: Decay rates (s^{-1}) for the ground state and yrast 2^+ state of ^{68}Se decomposed into the corresponding β^+ and electron capture components for selected densities ρY_e (mol/cm^3) as a function of temperature T (GK) obtained using the Bonn A (left) and Bonn CD (right) potential.

rp-process astrophysical environment electrons and positrons are well described by Fermi-Dirac distributions, with temperature T and chemical potential μ by

$$S_e = \frac{1}{exp[(E_e - \mu_e)/(kT)] + 1}, \qquad (7)$$

with $E_e = wm_ec^2$. The positron distribution is defined similarly with $\mu_p = -\mu_e$. The chemical potential, μ_e, is determined from the density ρ (in g/cm^3) inverting the relation

$$\rho Y_e = \frac{1}{\pi^2 N_A}\left(\frac{m_e c}{\hbar}\right)^3 \int_o^\infty (S_e - S_p)p^2 dp \qquad (8)$$

(in mol/cm^3), where Y_e is the electron-to-baryon ration (in mol/g), and N_A is Avogadro's number. The density of electron-positron pairs has been removed by forming the difference $S_e - S_p$. In the *rp*-process scenarios it is assumed that $S_\nu = 0$ and $S_p = 0$.

For the *rp*-process waiting point nucleus ^{68}Se we investigated the influence of shape coexistence and mixing on the stellar weak interaction rates taking into account the thermally populated yrast 2^+ state situated at 854 keV excitation energy. Experimentally 0^+ excited states are not identified, whereas the theoretical prediction indicates excitation ener-

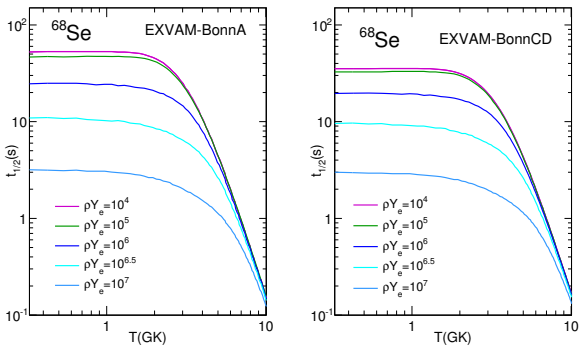

Figure 10: Half-lives (s) of ^{68}Se for selected densities ρY_e (mol/cm^3) as a function of temperature T (GK) obtained using Bonn A (left) and Bonn CD (right) potential.

gies higher than 1 MeV for the excited 0^+ states [4].

In Figure 8 we present the decay rates of ^{68}Se as a function of temperature T (GK) for a typical density $\rho Y_e = 10^6 mol/cm^3$ obtained within the *complex* Excited Vampir model using Bonn A and Bonn CD potential in the standard model space. The total rate, β^+ and continuum electron capture, is decomposed into contributions from the decay of the ground state of ^{68}Se to 1^+ states in the ^{68}As daughter nucleus and from the yrast 2^+ state to the daughter 1^+, 2^+, and 3^+ states. Similar general trends have been presented in the previous study [5], except for the contribution from the decay of the yrast 2^+ state to the 2^+ daughter states, negligible in our case as it is expected from the Gamow-Teller accumulated strengths presented in Figure 2.

In Figure 9 is illustrated the effect of the changes induced in the shape mixing replacing Bonn A by Bonn CD potential on the evolution of the decay rates as a function of temperature for selected densities ρY_e. The decay rates for the ground state and yrast 2^+ state of ^{68}Se are decomposed into the corresponding β^+ and continuum electron capture components. For the *rp*-process typical density $\rho Y_e = 10^6 mol/cm^3$ one can observe that for the results obtained using Bonn CD potential the electron capture ovecomes the β^+ component only at temperatures larger than 2 GK.

The results on the half-lives of ^{68}Se for selected densities ρY_e as a function of temperature for Bonn A and Bonn CD potential are compared in Figure 10. The induced differences in the oblate-prolate mixing for the parent as well as daughter states are responsible for a variation of 24% for the half-life obtained at T = 1.5 GK and $\rho Y_e = 10^6 mol/cm^3$.

The investigation of the *rp*-process waiting point nucleus ^{72}Kr included the termally populated first excited 0^+ state and yrast 2^+ state situated at 671 keV and 710 keV, respectively, different model spaces, standard and extended, and effective interactions obtained starting from Bonn A and Bonn CD potential.

In Figure 11 are presented the contributions to the decay rates from β^+ and continuum electron capture (at $\rho Y_e = 10^6 mol/cm^3$) as a function of temperature calculated in the extended model space using Bonn A potential. The total rate is decomposed into contributions from the decay of the ground state, first excited 0^+ state, and yrast 2^+ state to the daughter states in ^{72}Br.

The decay rates presented in Figure 12 as a function of temperature illustrate the effects of changes in the shape mixing underlying the structure of parent and daughter states evidenced in the GT accumulated strength (Figure 6) obtained in different model spaces using Bonn A potential. The total rate calculated at density $\rho Y_e = 10^6 mol/cm^3$ is decomposed into contributions from the decay of the ground state, first excited 0^+ state, and yrast 2^+ state to the daughter states in ^{72}Br. The results indicate that in the standard model space the contribution from the excited 0^+ state is much weaker than the contribution from the $2_1^+ \rightarrow 1^+$ and $2_1^+ \rightarrow 3^+$ decays. Different than the situation found in ^{68}Se the results obtained for ^{72}Kr in the standard and extended model space indicate almost identical behaviour for the total decay rate even if significant differences are revealed by the GT accumulated strength.

In Figure 13 are presented the total decay rates decomposed into the corresponding β^+ and electron capture components and the half-lives for selected densities ρY_e as a function of temperature obtained using Bonn A potential in the extended model space. The general trend is similar with the results obtained using QRPA model [5] even if the decomposition into the contributions from the parent states to various daughter states as well as the relative contribution from the β^+ and continuum electron capture indicate different behaviour.

This results represents the first beyond-mean-field treatment based on realistic effective interactions in rather large model spaces able to describe self-consistently the effect of shape coexistence and mixing on the stellar weak interaction rates in A$\sim$70 *rp*-process waiting point nuclei manifesting variable shape mixing with increasing spin and excitation energy [7]. The realistic description of the shape coexistence and mixing dominating the structure of the ^{68}Se and ^{72}Kr waiting points as well as the daughter ^{68}As and ^{72}Br nuclei, respectively, reveal different effects on the stellar decay rates at the *rp*-process typical conditions of temperature and densities. Maximum effect is obtained for ^{68}Se where a variation of 24% in the total decay rate at T = 1.5 GK and $\rho Y_e = 10^6 mol/cm^3$ is produced by changes in the shape mixing introduced replacing Bonn A by Bonn CD potential. Future experiments scheduled at ISOLDE for the investigation

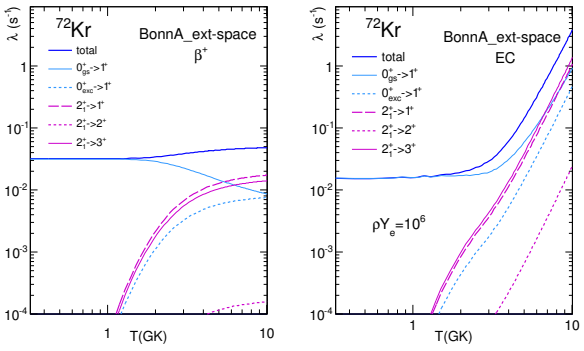

Figure 11: Decay rates (s^{-1}) of ^{72}Kr for β^+ (left) and continuum electron capture (right) as a function of temperature T (GK) obtained using Bonn A potential in the extended model space. The total rate is decomposed into contributions from the decay of the ground state, first excited 0^+ state, and yrast 2^+ state to the daughter states in ^{72}Br.

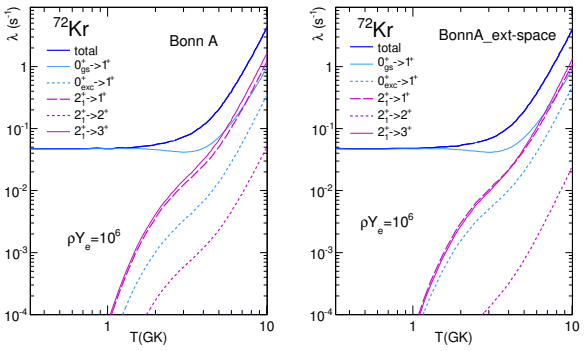

Figure 12: Decay rates (s^{-1}) for the ground state, first excited 0^+ state, and yrast 2^+ state of ^{72}Kr as a function of temperature T (GK) for *rp*-process typical density ρY_e (mol/cm^3) obtained using the Bonn A potential in the standard (left) and extended model space (right).

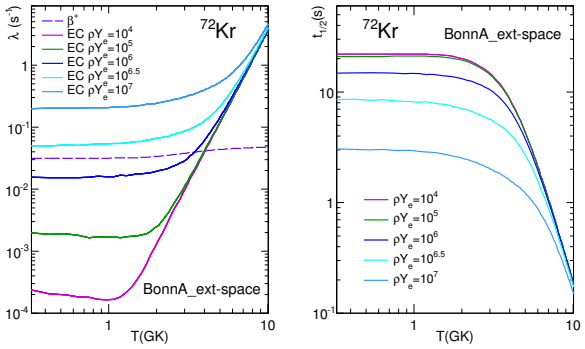

Figure 13: Decay rates (s^{-1})(left) of ^{72}Kr decomposed into the corresponding β^+ and electron capture components and half-lives (s) (right) for selected densities ρY_e (mol/cm^3) as a function of temperature T (GK) obtained using Bonn A potential in the extended model space.

of the Gamow-Teller strength distribution of ^{68}Se using the TAS spectrometer could test the theoretical predictions. Furthermore, the near-future measurements at RIKEN on electromagnetic properties of ^{72}Kr nucleus could help the beyond-mean-field models to improve the description of shape coexistence and mixing and, consequently, their effects on the stellar decay rates of the *rp*-process waiting point nuclei in the A$\sim$70 mass region.

References

[1] G. M. Fuller, W. A. Fowller, M.J. Newman, Astrophys. J. Suppl. Ser. **42**, 447 (1980).

[2] K. Langanke and G. Martinez-Pinedo, Rev. Mod. Phys. **75**, 819 (2003).

[3] A. Petrovici, K.W. Schmid, O. Radu, A. Faessler, Phys. Rev. C **78**, 044315 (2008).

[4] A. Petrovici, K.W. Schmid, O. Andrei, A. Faessler, Phys. Rev. C **80**, 044319 (2009).

[5] P. Sarriguren, Phys. Rev. C **83**, 025801 (2011).

[6] I. Piqueras *et al.*, Eur. Phys. J. A **16**, 313 (2003).

[7] A. Petrovici and O. Andrei, Eur. Phys. J. A **51**, 133 (2015).

II. Shape Coexistence and Shape Evolution in the N = 58 Kr Isotope

The oblate-prolate shape coexistence specific for each spin up to 10^+ and the evolution of the shape coexistence and mixing in the neutron-rich ^{94}Kr isotope are studied within the *complex* Excited Vampir approach using a realistic effective interaction based on Bonn CD potential in a large model space. The influence of the shape mixing on the structure and dynamics of the lowest few positive parity states is discussed and comparison to the available data is presented.

I. INTRODUCTION

The investigation of the neutron-rich nuclei in the A $\simeq$ 100 mass region is receiving an increasing interest both theoretically and experimentally [1]. The structure of these nuclei relevant for the astrophysical r-process manifests drastic changes in some isotopic chains and often sudden variations of particular nuclear properties have been identified. Neutron-rich Sr and Zr nuclei indicate rapid transition from spherical to deformed shape with a possible identification of triple shape coexistence in the N=58 ^{96}Sr and ^{98}Zr [2]. Previous theoretical investigations revealed the difficulty of describing the shape coexistence and shape transition suggested by the experimental data at low spins and the richness of various structural effects occuring at intermediate and high spins. For a realistic description of the evolution in structure with increasing energy, spin, and isospin determined by shape coexistence and mixing beyond-mean-field approaches are required.

The present study is an attempt to the self-consistent description of the shape coexistence phenomena in the neutron-rich ^{94}Kr isotope. Since the onset of deformation is supposed to take place for N > 58 we investigated the structural changes and the evolution of deformation with increasing spin aiming at a unitary description of the lowest few 0^+ states and the low and intermediate spins studied within the *complex* Excited Vampir (EXVAM) variational model with symmetry projection before variation using a realistic effective interaction and a large model space.

II. THEORETICAL FRAMEWORK

For nuclei in the A $\simeq$ 100 mass region is used a rather large model space above the ^{40}Ca core built out of $1p_{1/2}$, $1p_{3/2}$, $0f_{5/2}$, $0f_{7/2}$, $2s_{1/2}$, $1d_{3/2}$, $1d_{5/2}$, $0g_{7/2}$, $0g_{9/2}$, and $0h_{11/2}$ oscillator orbits for both protons and neutrons in the valence space. The corresponding single-particle energies (in units of the oscillator energy $\hbar\omega$) are 0.037, -0.173, 0.299, -1.090, 0.715, 0.932, 0.198, 1.524, 0.034, 1.186 for the proton, and -0.141, -0.292, 0.038, -1.220, 0.909, 1.044, 0.758, 1.384, -0.038, 0.873 for the neutron levels, respectively. The single particle energies had been adjusted in *complex* Monster(Vampir) calculations [2] for odd mass nuclei in the A $\simeq$ 100 mass region.

The effective two-body interaction is constructed from a nuclear matter G-matrix based on the Bonn CD potential. In order to enhance the pairing properties the G-matrix was modified by three short-range (0.707 fm) Gaussians for the isospin T = 1 proton-proton, neutron-neutron, and neutron-proton matrix elements with strengths of -40, -30, and -35 MeV, respectively. The isoscalar spin 0 and 1 particle-particle matrix elements are enhanced by an additional Gaussian with the same range and the strength of -70 MeV. In addition the isoscalar interaction was modified by monopole shifts for all T = 0 matrix elements of the form $\langle 0g_{9/2}0f; IT = 0|\hat{G}|0g_{9/2}0f; IT = 0\rangle$ involving protons and neutrons occupying the $0f_{5/2}$ and the $0f_{7/2}$ orbitals. The Coulomb interaction between the valence protons was added.

We calculated the lowest positive parity states up to spin 10^+ in ^{94}Kr including in the Excited Vampir many-nucleon bases up to 7 EXVAM configurations. The final solutions for each spin have been obtained diagonalizing the residual interaction between the considered Excited Vampir configurations. For each nucleus the calculated states have been organized in bands based on the B(E2;$\Delta I = 2$) values connecting them.

III. RESULTS AND DISCUSSION

The theoretical lowest bands of ^{94}Kr are compared to the experimental spectrum in Fig. 1. The good agreement with the available data gives support to our description of the structure of N=58 isotopes of ^{94}Kr, ^{96}Sr, and ^{98}Zr based on shape coexistence and mixing that requires beyond-mean-field theoretical models for a realistic description of the coexistence phenomena revealed by the experimental data. The labels of the bands indicate the prolate (p) or oblate (o) intrinsic quadrupole deformation for the dominant projected EXVAM configurations underlying the states of the corresponding bands. The states building the $op(p)$-band are characterized by strong prolate-oblate mixing at low spins and variable prolate mixing at intermediate spins.

The results concerning the oblate-prolate mixing in the structure of the wave functions for the lowest two states up to spin 6^+ and the lowest three states for spin 8^+ and 10^+ is illustrated in Table I. We indicate the contribution of the EXVAM configurations bringing at least 1% of the total amplitude.

Support for the mixing of configurations with different intrinsic deformations in the structure of the wave functions for the 0^+ states is offered by the strong $\rho^2(E0)$ values for the transition from the second to the lowest 0^+ state. At intermediate spins specific aspects of shape coexistence and mixing have been identified. The present

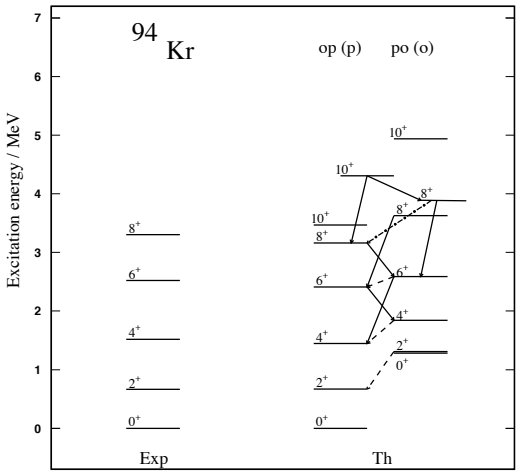

FIG. 1. The theoretical EXVAM spectrum of ^{94}Kr is compared to the experimental data [1].

TABLE I. The o-p mixing of the lowest calculated states.

I[$\hbar$]	o-mixing	p-mixing	I[$\hbar$]	o-mixing	p-mixing
0_1^+	62(4)%	32(2)%	8_1^+	1%	97(2)%
0_2^+	35(5)%	58(1)(1)%	8_2^+	92(3)(2)%	2(1)%
2_1^+	71(5)(1)%	22(1)%	8_3^+	3(2)%	87(7)(1)%
2_2^+	25%	74(1)%	10_1^+		80(19)(1)%
4_1^+	75(4)(1)%	19(1)%	10_2^+		63(15)(12)(9)%
4_2^+	20%	78%	10_3^+	94(4)(1)%	
6_1^+	40(3)(1)%	55(1)%			
6_2^+	58(1)%	40%			

investigations will be continued and our *complex* Excited Vampir results will be compared with the new data obtained within the EXILL colaboration at ILL Grenoble, France.

[1] T. Rzaca-Urban *et al.*, Eur. Phys. J. A **9**, 165 (2000).

[2] A. Petrovici, Phys. Rev. C **85**, 034337 (2012).

Project leader,
Alexandrina Petrovici